2011

Laser Propagation in Biaxial Liquid Crystal Polymers

Choate, Eric P.

Laser Propagation in Biaxial Liquid Crystal Polymers

Eric P. Choate[1] **and Hong Zhou**

Department of Applied Mathematics,
Naval Postgraduate School, Monterey, CA

Abstract

We examine the propagation of a laser beam through a liquid crystal polymer (LCP) layer using the finite-difference time-domain (FDTD) method. Anchoring conditions on supporting glass plates induce an orientational structure in the LCP between the plates. The orientation can deflect energy away from the direction of propagation of the incident beam when the optical axis or major director of a uniaxial medium is neither parallel nor orthogonal to the incident beam. The maximum energy deflection occurs when the angle between the incident beam and the major director of the orientation is 45 degrees, but for spatially uniform orientations, polarization orthogonal to the plane containing the major director and the propagation direction is unaffected. We investigate how to overcome this by twisting the anchoring alignment on the plates with respect to each other to generate a helical structure in the orientation across the gap to deflect all polarizations. We also examine the difference between the commonly used Leslie-Ericksen theory for the LCP, which assumes a uniaxial orientation, and the more general Doi-Marrucci-Greco orientation tensor model, which allows for both biaxial structures and oblate defect phases.

Keywords: Liquid crystal polymers, Laser propagation in anisotropic media, Finite-Difference Time-Domain method

Nomenclature

$\mathbf{D}$ = electric displacement field
$\mathbf{E}$ = electric field
$\mathbf{H}$ = magnetic field
$\mathbf{n}$ = major director of the LCP orientation
$\boldsymbol{\varepsilon}$ = permittivity tensor
$\varepsilon_\perp$ = ordinary permittivity
$\varepsilon_{||}$ = extraordinary permittivity
$\mathbf{I}$ = identity tensor
h = gap width
λ_0 = free space wavelength of the incident beam

[1]Corresponding author: Department of Applied Mathematics, Naval Postgraduate School, 833 Dyer Rd, Bldg 232, SP-250, Monterey, CA, 93943. Phone: 831-656-3247. Fax: 831-656-2355. Email: echoate@nps.edu.

$k_\perp$ = ordinary wave number
k_θ = effective extraordinary wave number
ψ = azimuthal director angle
θ = elevation director angle

Introduction

Liquid crystal displays have become commonplace due to the dynamic controllability of the anisotropic refractive indices of the liquid crystals. In our previous work in one-dimensional systems [Choate and Zhou, 2011], we examined propagation of a plane wave across a liquid crystal polymer (LCP) layer using the finite-difference time-domain (FDTD) method, and we paid special attention to the dependence of the transmitted intensity on the orientation as controlled by the anchoring conditions on the supporting glass layers. In this paper, we retain the one-dimensional heterogeneity in the orientation, but we move to a three-dimensional electromagnetic system so that we can examine laser propagation across an LCP layer. This allows us to examine the possibility of deflecting the beam away from the direction of propagation of the incident beam.

Motivated by a one-dimensional analytical calculation for plane waves in a homogeneous anisotropic medium, we find that a Gaussian beam can be deflected if the anchoring orientation is neither parallel nor orthogonal to the supporting plates. The maximum deflection occurs when the polarization of the incident beam matches the projection of the major director onto the supporting glass plates, but in this case, a different incident beam with an orthogonal polarization will not be deflected. We examine how to rotate the anchoring conditions to induce a twisting helical structure in the orientation so that all incident polarizations are deflected.

Model setup and theory

We consider the propagation of Gaussian beam across an LCP medium. The incident beam is a monochromatic wave with a wavelength of $\lambda_0 = 633$ nm. The waist of the Gaussian beam has a radius of $1.5\lambda_0$, and it propagates in the z-direction with the polarization of its electric field in the x-direction. The beam passes through a lower supporting glass plate at $z = 0$, and then through an LCP layer of width $h = 10\lambda_0$, and then through a second glass plate. In order to focus on the effect of the anisotropy of the LCP, we assign the relative permittivity and relative permeability of the glass plates to be 1.

The inside surfaces of both glass plates are mechanically rubbed to impose anchoring conditions that align the major director or optical axis $\mathbf{n}$, the most preferred direction of the alignment of the LCP molecules, which we model as high aspect ratio spheroids. If we use different anchoring conditions on the two plates, we can create orientational structures across

the LCP domain with gradients in the optical axes that can refract light in a controlled way. In this paper, we assume uniform anchoring in the x- and y-directions so that the structure varies only in the z-direction. We assume that the orientation is unaffected by the passage of the beam through it.

One of the goals of our research is to probe the differences in the light propagation due to the choice of model used to describe the structure of the molecular alignment imposed by these anchoring conditions across the layer. Leslie-Ericksen (LE) continuum theory tries to predict only the major director $\mathbf{n}(\mathbf{x})$, while the more complex Doi-Marrucci-Greco (DMG) tensor theory also provides information about the shape of the orientational distribution around that preferred direction through the second moment tensor $\mathbf{M}(\mathbf{x})$ of a molecular probability density function [Wang, 2002]. This allows the DMG model to capture states such as the defect states, including the isotropic case, in which there is no preferred direction of alignment, and also biaxial cases in which the projections of the molecules onto the plane orthogonal to the major director show a preference for a second direction. For the anchoring conditions we examine in this paper, however, the biaxiality is negligible, and so effectively, the DMG theory predicts that the second moment tensor is $\mathbf{M} = s_0(\mathbf{nn}-\frac{\mathbf{I}}{3})+\frac{\mathbf{I}}{3}$, where $\mathbf{n}$ is the major director predicted from LE theory, $\mathbf{I}$ is the identity tensor, and $s_0 = \frac{1}{4}(1+3\sqrt{1-\frac{8}{3N}})$ is the equilibrium order parameter for the nondimensional concentration parameter N, which measures the strength of the excluded volume potential.

In LE theory, the orientation is described by a single unit vector field $\mathbf{n}(\mathbf{x})$ called the major director, which gives the average direction of the axes of symmetry $\mathbf{m}$ of the molecules located at $\mathbf{x}$. The molecules are assumed to have a fore-aft symmetry and so there is no distinction between $\mathbf{n}$ and $-\mathbf{n}$. In the absence of flow and neglecting reorientation by the electromagnetic field, $\mathbf{n}$ is governed by the steady-state equation [de Gennes and Proust, 1993]

$$\mathbf{0} = (\mathbf{I} - \mathbf{nn}) \cdot \nabla^2 \mathbf{n}. \tag{1}$$

We parameterize $\mathbf{n}$ with the azimuthal director angle ψ and the elevation director angle θ as

$$\mathbf{n}(z) = \begin{bmatrix} \cos\theta\cos\psi \\ \cos\theta\sin\psi \\ \sin\theta \end{bmatrix}, \tag{2}$$

so that (1) becomes

$$\begin{aligned} \nabla^2\theta + \sin\theta\cos\theta\nabla\psi\cdot\nabla\psi &= 0, & (3)\\ \nabla^2\psi - 2\tan\theta\nabla\psi\cdot\nabla\theta &= 0. & (4) \end{aligned}$$

The anchoring conditions supply the boundary conditions for these equations as $(\theta_{bottom}, \psi_{bottom})$ at the bottom plate ($z = 0$) and $(\theta_{top}, \psi_{top})$ at the top plate ($z = h$). If we apply the same

anchoring conditions on each plate, $(\theta_{bottom}, \psi_{bottom}) = (\theta_{top}, \psi_{top})$, then these extend across the gap, and we have a homogeneous solution we denote by (θ_0, ψ_0). If $\theta_{bottom} = \theta_{top} = 90°$, we have a homogeneous orientation that is orthogonal to the plates. If $\theta_{bottom} = \theta_{top} = 0°$, we have parallel anchoring, and the director is parallel to the plates across the gap, with a linear interpolation for $\psi(z)$ between its anchoring conditions, which creates a helical structure called a twist. If $\theta_{bottom} = \theta_{top}$ but not equal to either 0° or 90°, then in addition to a possible twist in $\psi(z)$, $\theta(z)$ can vary in what is known as a splay orientation.

The LCP orientation enters the electrodynamics through the anisotropic permittivity tensor, which for the LE model is

$$\boldsymbol{\varepsilon}_{LE} = \varepsilon_{\perp}\mathbf{I} + \Delta\varepsilon\mathbf{nn} \tag{5}$$

where $\Delta\varepsilon = \varepsilon_{||} - \varepsilon_{\perp}$, for the extraordinary permittivity constant $\varepsilon_{||}$ for the direction parallel to the major director and the ordinary permittivity constant $\varepsilon_{\perp}$ for the orthogonal directions. We adopt the permittivity values $\varepsilon_{||} = 2.89\varepsilon_0$ and $\varepsilon_{\perp} = 2.25\varepsilon_0$ from [Hwang and Rey, 2005a,b, 2006]. The DMG permittivity tensor takes a similar form, $\boldsymbol{\varepsilon}_{DMG} = \varepsilon_{\perp}\mathbf{I} + \Delta\varepsilon\mathbf{M}$. Both models assume the relative permeability is 1.

To solve Maxwell's equations, we use the Finite-Difference Time-Domain (FDTD) method to advance the electromagnetic field [Taflove and Hagness, 2005; Hwang and Rey, 2005a,b, 2006; Hwang, et al.; Kriezis and Elston, 1999, 2000]. This is due to its ability to handle spatial gradients in the molecular orientation better than previous methods. Due to the nature of the staggered grid used by the FDTD method to store some elements of $\mathbf{D}, \mathbf{E}$, and $\mathbf{H}$ on the grid and others on the half-grid, care must be taken when we invert $\boldsymbol{\varepsilon}$ in the constitutive equation in our loop. We use

$$Dx^{n+1}_{i+1/2,j,k} = Dx^{n}_{i+1/2,j,k} + \Delta t(\nabla \times \mathbf{H})^{n+1/2}_{x,i+1/2,j,k}, \tag{6}$$

$$\begin{aligned} Ex^{n+1}_{i+1/2,j,k} = {} & \varepsilon x x^{-1}_{i+1/2,j,k} Dx^{n+1}_{i+1/2,j,k} \\ & + \frac{1}{4}\varepsilon x y^{-1}_{i+1/2,j,k}(Dy^{n+1}_{i,j+1/2,k} + Dy^{n+1}_{i+1,j+1/2,k} + Dy^{n+1}_{i,j-1/2,k} + Dy^{n+1}_{i+1,j-1/2,k}) \\ & + \frac{1}{4}\varepsilon x z^{-1}_{i+1/2,j,k}(Dz^{n+1}_{i,j,k+1/2} + Dz^{n+1}_{i+1,j,k+1/2} + Dz^{n+1}_{i,j,k-1/2} + Dz^{n+1}_{i+1,j,k-1/2}), \end{aligned} \tag{7}$$

$$Hx^{n+3/2}_{i,j+1/2,k+1/2} = Hx^{n+1/2}_{i,j+1/2,k+1/2} - \frac{\Delta t}{\mu_0}(\nabla \times \mathbf{E})^{n+1}_{x,i,j+1/2,k+1/2}, \tag{8}$$

and similar equations for the other field components.

We use a scattered field/total field formulation to introduce the incident beam at the lower boundary of the total field region, and we use uniaxial perfectly matched layers to truncate the computational domain without creating artificial reflections.

Direct comparison of Leslie-Ericksen and Doi-Marrucci-Greco models

Before we solve the system for the propagation, there is one direct comparison of the LE and DMG models to be made. If we apply the same anchoring conditions on both plates, $\mathbf{n}_{top} = \mathbf{n}_{bottom} = \mathbf{n}_0$, an arbitrary unit vector, then the LE theory yields $\boldsymbol{\varepsilon}_{LE} = \varepsilon_\perp \mathbf{I} + \Delta\varepsilon \mathbf{n}_0\mathbf{n}_0$, and the DMG theory gives

$$\begin{aligned} \boldsymbol{\varepsilon}_{DMG} &= \varepsilon_\perp \mathbf{I} + \Delta\varepsilon(s_0(\mathbf{n}_0\mathbf{n}_0 - \frac{\mathbf{I}}{3}) + \frac{\mathbf{I}}{3}) && (9) \\ &= (\varepsilon_\perp + \Delta\varepsilon\frac{1-s_0}{3})\mathbf{I} + s_0\Delta\varepsilon\mathbf{n}_0\mathbf{n}_0. && (10) \end{aligned}$$

Here we can readily identify effective extraordinary and ordinary permittivities for the DMG model as functions of the extraordinary and ordinary permittivities and the equilibrium order parameter as

$$\begin{aligned} \varepsilon_\perp^{eff} &= \varepsilon_\perp + \Delta\varepsilon\frac{1-s_0}{3} = \varepsilon_\perp\frac{2+s_0}{3} + \varepsilon_{||}\frac{1-s_0}{3}, && (11) \\ \Delta\varepsilon^{eff} &= s_0\Delta\varepsilon, && (12) \\ \varepsilon_{||}^{eff} &= \Delta\varepsilon^{eff} + \varepsilon_\perp^{eff} = \varepsilon_{||}\frac{2s_0+1}{3} + \varepsilon_\perp\frac{2(1-s_0)}{3}. && (13) \end{aligned}$$

Since s_0 is a function of the concentration parameter N, the effective permittivities are also functions of N. In the infinite concentration limit, the effective permittivities approach the LE values, which is consistent with the LE formulation being the infinite concentration limit of DMG theory. For finite concentrations in the nematic regime, the DMG model effectively decreases the uniaxial anisotropy.

Motivation from 1D analytical solution

An important motivation is found by looking at the situation in which the same anchoring conditions are applied at both the top and bottom plates so that the major director is parameterized by the constant angles ψ_0 and θ_0 as

$$\mathbf{n}(z) = \begin{bmatrix} \cos\theta_0\cos\psi_0 \\ \cos\theta_0\sin\psi_0 \\ \sin\theta_0 \end{bmatrix}. \quad (14)$$

The plane waves supported by such a layer can be found analytically as

$$\mathbf{E} = C_\perp\mathbf{E}_\perp + C_\theta\mathbf{E}_\theta, \quad \mathbf{H} = C_\perp\mathbf{H}_\perp + C_\theta\mathbf{H}_\theta, \quad (15)$$

for the set of basis vectors

$$\mathbf{E}_\perp = \begin{bmatrix} -\sin\psi_0 \\ \cos\psi_0 \\ 0 \end{bmatrix} e^{i(k_\perp z - \omega t)}, \quad \mathbf{H}_\perp = \sqrt{\frac{\varepsilon_\perp}{\mu_0}} \begin{bmatrix} -\cos\psi_0 \\ -\sin\psi_0 \\ 0 \end{bmatrix} e^{i(k_\perp z - \omega t)}, \quad (16)$$

where $k_\perp = \omega\sqrt{\varepsilon_\perp \mu_0}$, and

$$\mathbf{E}_\theta = \frac{1}{\bar{\varepsilon}_2}\begin{bmatrix} \bar{\varepsilon}_1 \cos\psi_0 \\ \bar{\varepsilon}_1 \sin\psi_0 \\ -\Delta\varepsilon \sin\theta_0 \cos\theta_0 \end{bmatrix} e^{i(k_\theta z - \omega t)}, \quad \mathbf{H}_\theta = \sqrt{\frac{\varepsilon_\perp}{\mu_0}}\frac{\sqrt{\varepsilon_{||}\bar{\varepsilon}_1}}{\bar{\varepsilon}_2}\begin{bmatrix} -\sin\psi_0 \\ \cos\psi_0 \\ 0 \end{bmatrix} e^{i(k_\theta z - \omega t)}, \quad (17)$$

where $k_\theta = \omega\sqrt{\frac{\varepsilon_\perp \varepsilon_{||}\mu_0}{\bar{\varepsilon}_1}}$, and $\bar{\varepsilon}_1 = \varepsilon_\perp \cos^2\theta_0 + \varepsilon_{||}\sin^2\theta_0$ and $\bar{\varepsilon}_2 = \sqrt{\varepsilon_\perp^2 \cos^2\theta_0 + \varepsilon_{||}^2 \sin^2\theta_0}$ are two weighted-average permittivities.

The Poynting vector for this wave is

$$\begin{aligned} \mathbf{E}\times\mathbf{H} \;&= \sqrt{\tfrac{\varepsilon_\perp}{\mu_0}}\begin{bmatrix} 0 \\ 0 \\ C_\perp^2 e^{2i(k_\perp z - \omega t)} + C_\theta^2 \frac{\sqrt{\bar{\varepsilon}_1^3 \varepsilon_{||}}}{\bar{\varepsilon}_2^2} e^{2i(k_\theta z - \omega t)} \end{bmatrix} + \\ &\sqrt{\tfrac{\varepsilon_\perp}{\mu_0}}\frac{\Delta\varepsilon \sin\theta_0 \cos\theta_0}{\bar{\varepsilon}_2}\begin{bmatrix} C_\theta C_\perp \sin\psi_0 e^{i((k_\perp + k_\theta)z - 2\omega t)} - C_\theta^2 \frac{\sqrt{\bar{\varepsilon}_1 \varepsilon_{||}}}{\bar{\varepsilon}_2}\cos\psi_0 e^{2i(k_\theta z - \omega t)} \\ -C_\theta C_\perp \cos\psi_0 e^{i((k_\perp + k_\theta)z - 2\omega t)} - C_\theta^2 \frac{\sqrt{\bar{\varepsilon}_1 \varepsilon_{||}}}{\bar{\varepsilon}_2}\sin\psi_0 e^{2i(k_\theta z - \omega t)} \\ 0 \end{bmatrix}. \end{aligned} \quad (18)$$

The important part of this is the overall factor of $\sin\theta_0 \cos\theta_0$ in the x- and y- components. Thus, if energy is to be deflected from the direction of propagation of the incident beam, the anchoring major director cannot be either parallel or orthogonal to the incident beam. Furthermore, it suggests the maximum deflection would occur when the anchoring of major director has $\theta_0 \approx 45°$. However, this assumes that C_θ is nonzero. If the incident beam polarized so that $C_\theta = 0$, then there is no deflection.

Numerical results

We begin our numerical investigation by examining the isotropic case with the same permittivity equal to the ordinary permittivity $\varepsilon_\perp$ of the following anisotropic cases. The transmitted intensity of the beam (scaled by $\sqrt{\frac{\varepsilon_\perp}{\mu_0}}$) is shown in Figure 1. Under this scaling, the peak intensity of the incident beam is 0.5, and in all of the following cases, we observed a peak intensity of slightly less than one-half the peak intensity of the incident beam. Figure 1 also shows the anisotropic case but with the major director $\mathbf{n}$ is uniformly orthogonal to the plates. That is, the extraordinary optical direction is aligned with the direction of propagation of the incident beam, and in the plane orthogonal to the incident beam, the anisotropic sample is effectively isotropic. The crosshairs show the peak of the incident beam, and so neither the isotropic or the orthogonal cases show any beam deflection. The orthogonal case does however compress the profile of the beam slightly in the direction of the polarization (the x-axis), but the cases are similar.

Next, we wanted to examine the effect of parallel anchoring (that is, anchoring orthogonal to the direction of propagation of the incident beam) with homogeneous orientations rotated

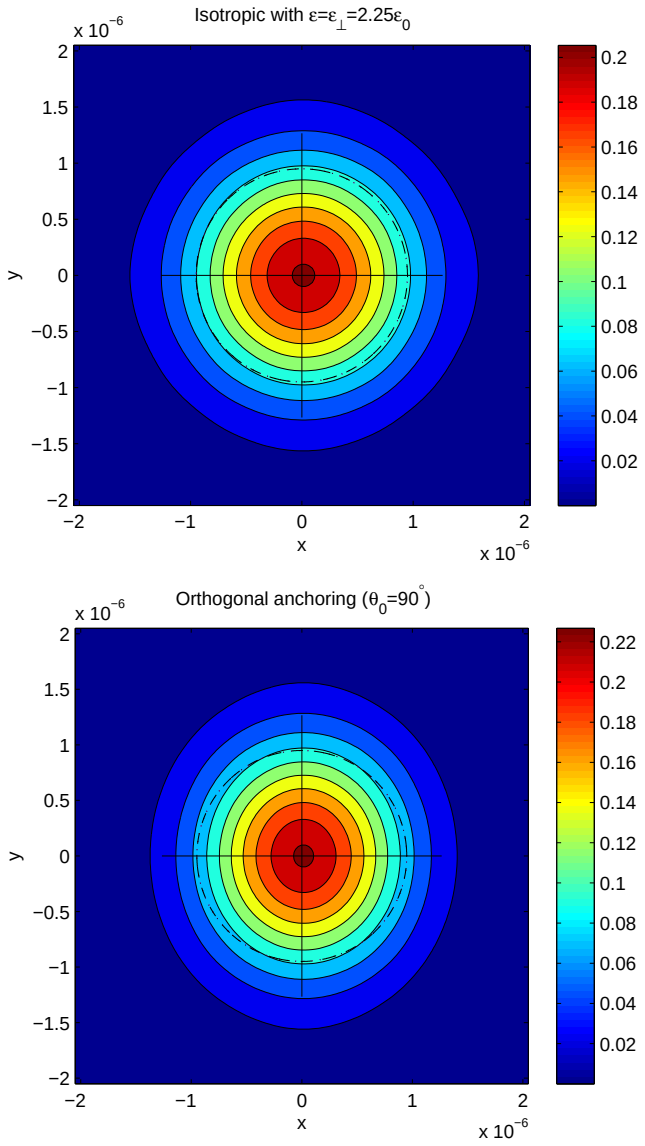

Figure 1: Transmitted intensity of a Gaussian beam passing through an isotropic sample with the same permittivity as the ordinary permittivity as the following anisotropic cases, $\varepsilon_\perp = 2.25\varepsilon_0$, compared with the anisotropic case with orthogonal anchoring.

with respect to the polarization of the incident beam. Figure 2 shows the (scaled) transmitted intensity for orientations aligned with the polarization, rotated 45° from the polarization, and aligned against the polarization. No case shows any deflection. The profile is stretched in the direction of the major director, but this effect is strongest when the major director is aligned with the polarization and nonexistent when aligned against the polarization.

We also examined twisted orientations in which the major director is always parallel to the plates across the gap, but the anchoring directors are orthogonal to each other. Effectively, this type of twist exposes every possible incident polarization to be aligned with some portion of the LCP layer. Figure 3 shows the transmitted intensity for the twists with $\psi_{bottom} = 0°$ to $\psi_{top} = 90°$, $\psi_{bottom} = 90°$ to $\psi_{top} = 0°$, and $\psi_{bottom} = -45°$ to $\psi_{top} = 45°$. As we expected, none of them show any deflection although they do rotate the polarization.

Now, we apply tilted anchoring conditions that the analytical plane wave calculations above suggest should show some beam deflection. Figure 4 shows three cases with homogeneous orientations so that the major director is tilted $\theta_0 = 30°, 45°$, and $60°$ with respect to the plates. All three show some deflection with 45° showing the largest deflection, with the peak intensity approximately deflecting 1.2 wavelengths from the path of the incident beam. This occurs over a layer that is 10 wavelengths across. Our preliminary studies show that the deflection increases approximately linearly with the width of the layer.

However, for each of the homogeneous layers of tilted anchoring shown in Figure 4, the projection of the major director onto the plane transverse to the direction of propagation of the beam is aligned with the polarization. Figure 5 compares two cases of homogeneous orientations that are tilted with $\theta_0 = 45°$, one in which the projection of the major director is aligned with the polarization and one in which the projection is orthogonal to the polarization. In this second case, there is no deflection. The farther the projection is from the polarization, the less the beam will deflect.

This can be overcome by twisting the anchoring conditions 90° with respect to each other so that any polarization will be aligned with the projection of the major director at some point across the layer. Thus, any incident beam will be deflected to some degree. Figure 6 shows twists with $\psi_{bottom} = 0°$ to $\psi_{top} = 90°$, $\psi_{bottom} = 90°$ to $\psi_{top} = 0°$, and $\psi_{bottom} = -45°$ to $\psi_{top} = 45°$ combined with the tilted anchoring conditions $\theta_{bottom} = \theta_{top} = 45°$. All of these heterogeneous orientations will deflect any polarization, but for each of them, some polarizations will be more deflected than others, and no polarization will be deflected as much as the homogeneous tilted anchoring from Figure 4. In addition to deflecting the beam, the twisted structures can rotate the polarization of the incident beam. Figure 7 shows the E_x and E_y components across the layer for the case with $\psi_{bottom} = 0°$ to $\psi_{top} = 90°$. It initially matches the polarization of the incident beam and then rotates to be polarized with the y-axis in addition to deflecting the beam.

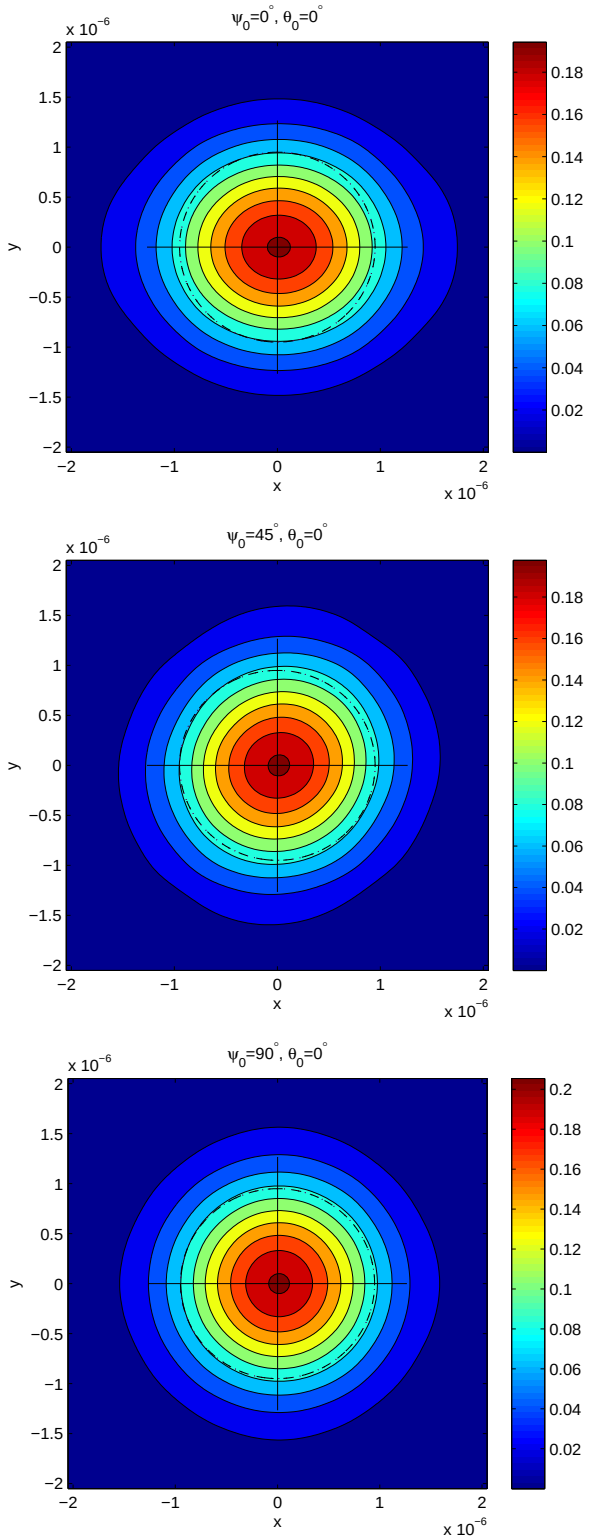

Figure 2: Homogeneous orientations with parallel anchoring aligned with the polarization ($\psi_0 = 0°$), rotated half-way ($\psi_0 = 45°$), and aligned against the polarization ($\psi_0 = 90°$).

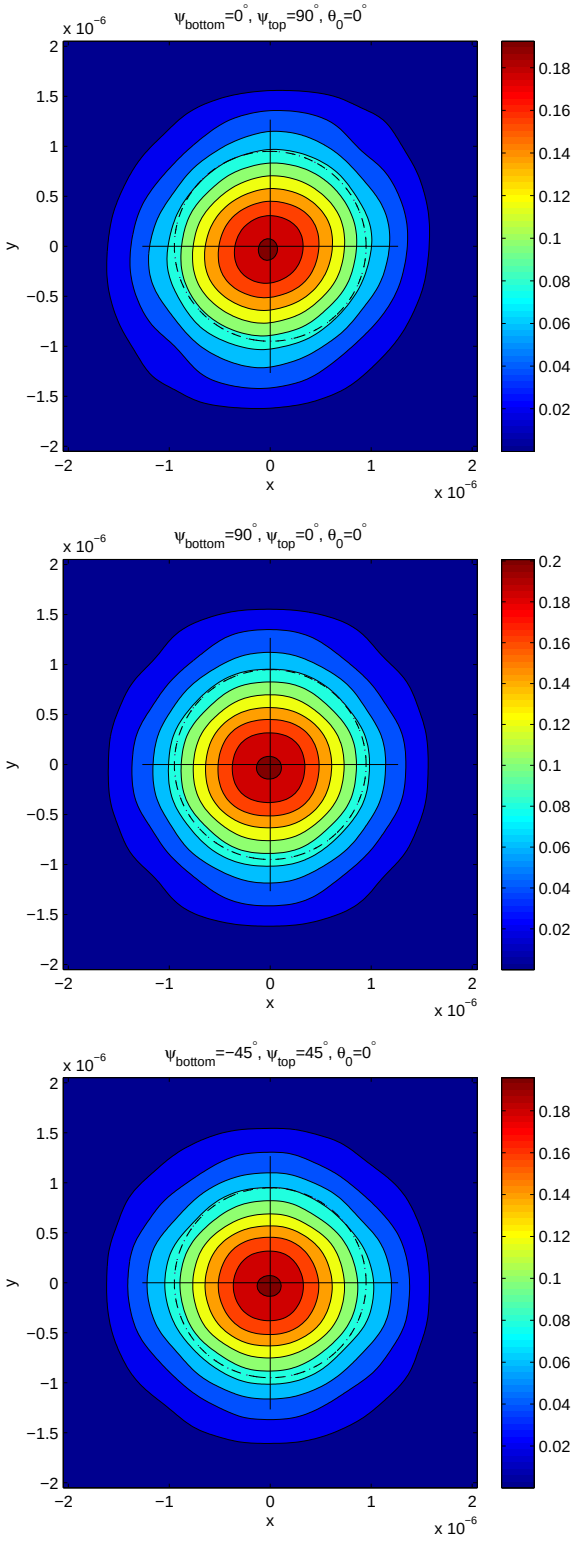

Figure 3: Parallel anchoring with three different twists.

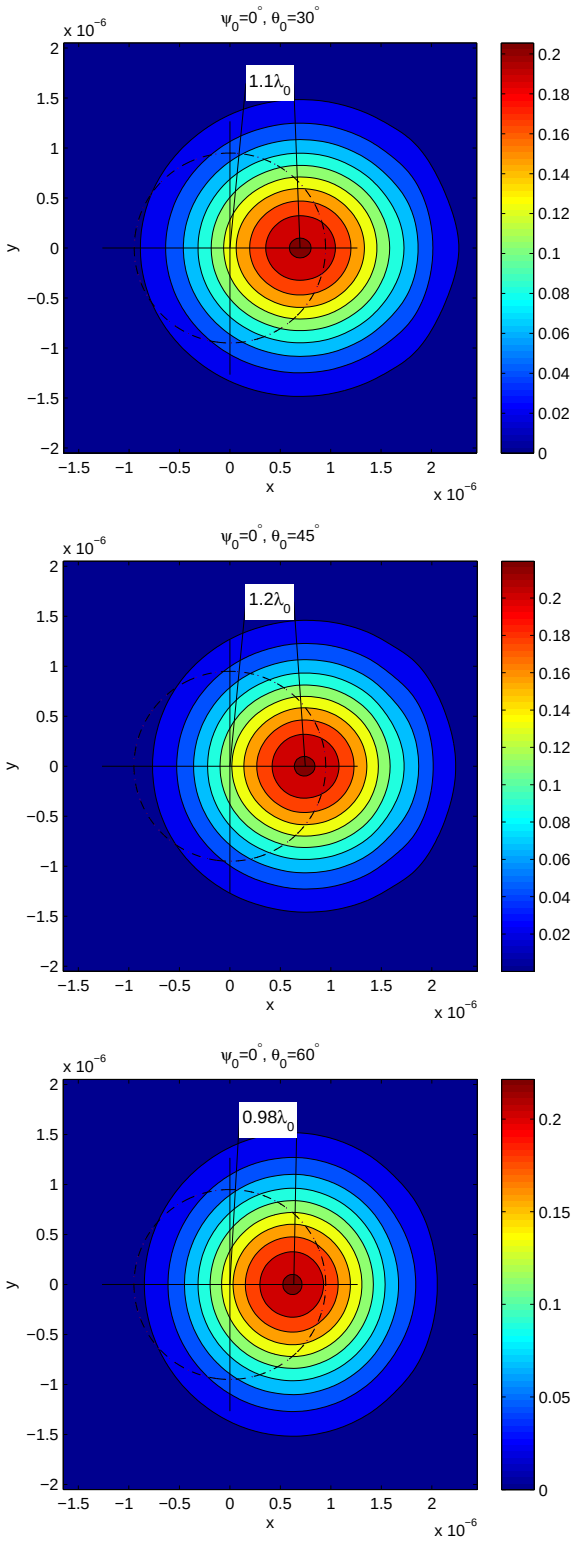

Figure 4: Transmitted intensities of homogeneous orientations with anchoring tilted $\theta_0 = 30°, 45°$, and $60°$ with respect to the plates.

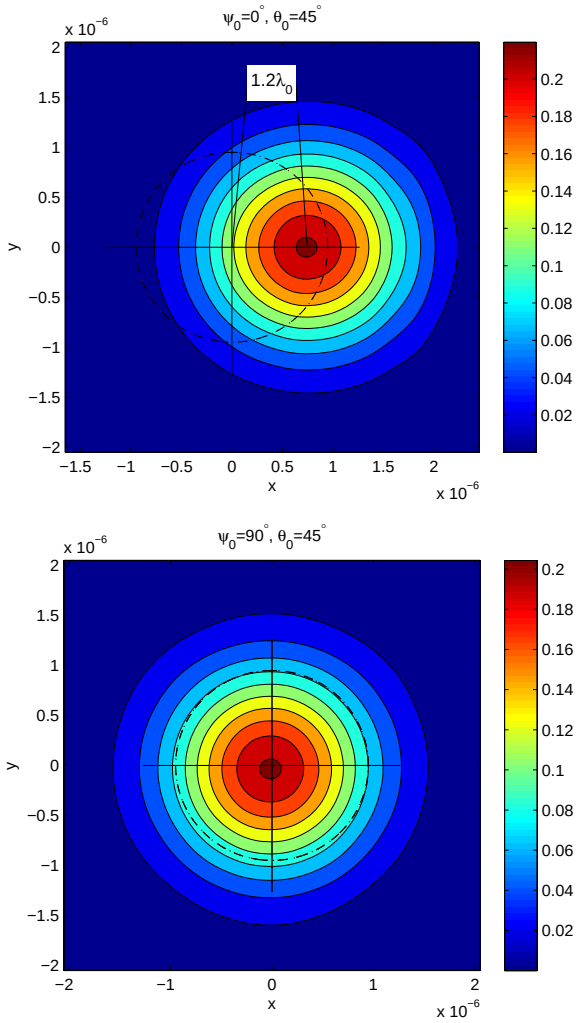

Figure 5: No deflection when the polarization is not aligned with the projection of the major director.

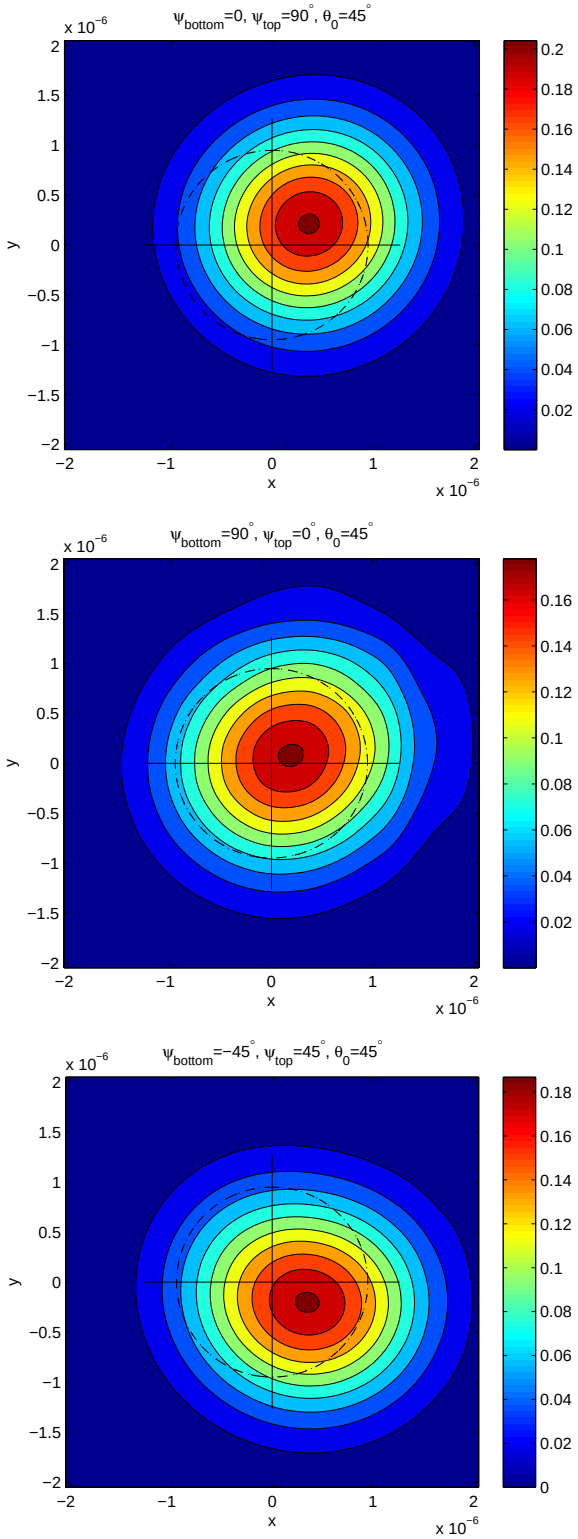

Figure 6: Tilted anchoring with three different twists. Each twist will deflect all polarizations to some degree.

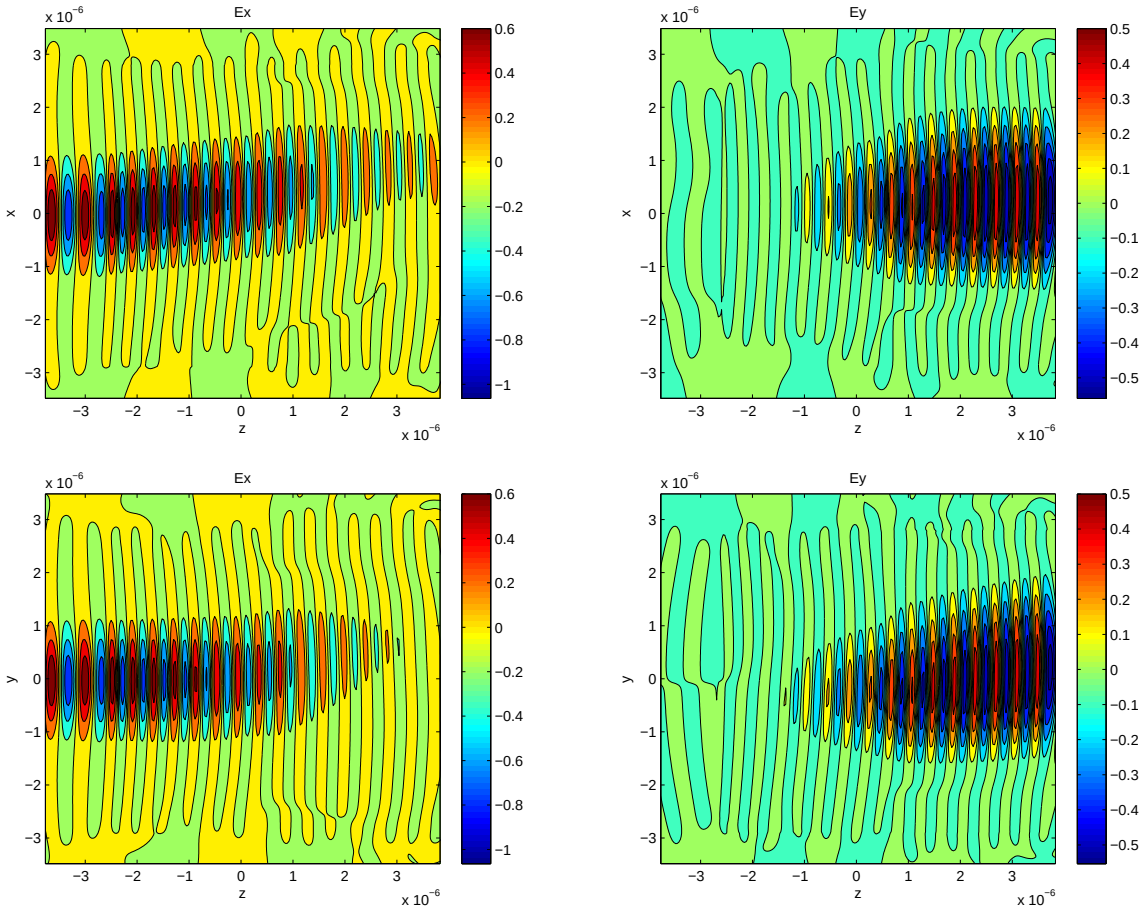

Figure 7: Slices of E_x and E_y across the layer for tilted anchoring with $\theta_{bottom} = \theta_{top} = 45°$ and twisting from $\psi_{bottom} = 0°$ to $\psi_{top} = 90°$. This orientation both deflects of the Gaussian beam and also the rotates of its polarization from E_x to E_y.

Conclusions and future work

We can deflect a beam with a liquid crystal polymer layer if the anchoring conditions induce an angle between the major director and the direction of propagation of the incident beam that is neither parallel nor orthogonal. The maximum deflection occurs approximately when this angle is approximately 45° and aligned with the polarization of the beam. All beams can be deflected if the anchoring directors are twisted 90° with respect to each other. We are continuing this preliminary work in order to find the exact values of the anchoring conditions to maximize the deflection both of a homogeneous system with the director aligned with the polarization and also for the twisted structure that can deflect all beams. We also wish to examine the effect of the thickness of the layer. Also, stacked layers of different homogeneous orientations rotated with respect to each other may show a way to combine the larger deflection of a homogeneous orientation with the ability of a twisted structure to deflect all beams. Additionally, we would like to study three-dimensional variations in the orientation including radial distributions and also biaxial structures.

Acknowledgements

This work was supported by a grant from the Office of Naval Research. It was also conducted while the author Eric P. Choate held a National Research Council Postdoctoral Research Associateship at the Department of Applied Mathematics at the Naval Postgraduate School.

References

Eric P. Choate and Hong Zhou, in preparation (2011)

Dae Kun Hwang and Alejandro D. Rey, Applied Optics, **44**, 4513 (2005a)

Dae Kun Hwang and Alejandro D. Rey, Liq. Cryst., **32**, 483 (2005b)

Dae Kun Hwang and Alejandro D. Rey, J. Opt. Soc. Am. A, **23**, 483 (2006)

Dae Kun Hwang and Alejandro D. Rey, J. Non-Newtonian Fluid Mech., **143**, 10 (2007)

Emmanouil E. Kriezis and Steve J. Elston, Optics Communications. **165**, 99 (1999)

Emmanouil E. Kriezis and Steve J. Elston, Optics Communications. **177**, 69 (2000)

Pierre-Gilles de Gennes and Jacques Prost. The Physics of Liquid Crystals. (Oxford University Press, 1993)

Allen Taflove and Susan C. Hagness, Computational Electrodynamics: The Finite-Difference Time Domain Method, 3rd ed. (Artech House, Boston, 2005)